THE EFFECT OF DISTORTION OF SUB-CAVITATING FOIL CONTOURS ON CAVITATION INCEPTION VELOCITY

BY

LTJG GEORGE P. MOECKEL

DAVID TAYLOR MODEL BASIN

WASHINGTON, D.C.

20007

OCTOBER 1965

LIST OF SYMBOLS

c	-	chord length of the foil section
C_P	-	pressure coefficient $\frac{P-P_\infty}{\frac{1}{2}\rho U^2}$
C_{P_i}	-	pressure coefficient at cavitation inception
P	-	local pressure on foil contour
P_A	-	atmospheric pressure
P_V	-	vapor pressure
P_∞	-	free stream pressure
U	-	free stream velocity
U_i	-	cavitation inception velocity
V	-	local velocity of fluid on the foil contour
x/c	-	station coordinate measured from the leading edge of the section to the trailing edge.
Y	-	offset coordinate of undistorted foil section measured as Y/c
Y_N	-	new offset coordinate of distorted foil section divided by the chord c
α	-	angle of incidence
ΔC_{P_i}	-	change of cavitation pressure coefficient due to the distortion
$\frac{\Delta t}{c}$	-	maximum variation in offset due to the distortion
ΔU_i	-	change in cavitation inception velocity due to the distortion
ΔY_N	-	change in offset coordinate divided by the chord c

LIST OF FIGURES

LIST OF FIGURES (continued)

ABSTRACT

The purpose of this paper is to investigate the theoretical effect of distortions on subcavitating foil sections in regard to cavitation inception velocities. The study is intended to give some prediction as to type and size of distortions that may be tolerated in foil construction. It is natural to expect errors in foil shape to occur as a result of inaccurate construction or damage. It is therefore the intention of this paper to provide estimates of admissible deviations from the intended foil geometry in order that cavitation may be prevented or at least anticipated.

INTRODUCTION

Some possible distortions were developed with respect to a single reference section. The reference section was an NACA 16-X08; X = .390. Theory was restricted to two-dimensional potential flow with circulation in an infinite fluid. Pressures were determined by a Douglas Aircraft Co. computer program for the solution of the Neumann problem extended to lifting infinite cascades, using a cascade spacing of zero which in this program specifies the special case of an isolated foil in an infinite fluid. (References 1 and 2)

The method of solution of the Neumann problem used in this paper is the application of a source distribution on the contour of the foil section under consideration such that the Neumann boundary condition is satisfied on the contour. This solution is obtained for uniform flow parallel to the chord, uniform flow perpendicular to the chord, and for vortex flow where a

vortex of unit strength is located in the interior of the contour. These three solutions are then superimposed at the desired angle of incidence such that the Kutta condition is satisfied at the trailing edge.

The pressure distribution was first calculated for an undistorted 16-X08 section with angle of incidence $-5.00^{\circ} \leq \alpha \leq +10.00^{\circ}$. For the purpose of defining certain distortions to compare with the undistorted section, about 290 stations were selected to define the foil geometry. All distortions considered were applied to the upper contour of the foil.

The distortions that were constructed may be placed in three categories: (1) general distortions, (2) flattening, (3) warping. The meaning of these terms shall be described in some detail. (1) By general distortions, it is meant that variations are applied to the entire foil, as opposed to local variations, so that the foil is completely altered from its originally intended geometry. To this end, a "bulge" was introduced at mid-chord and faired into the leading edge and tail. Also the foil was bulged at .25 x/c and dented at .75 x/c; these distortions likewise were faired into the leading edge, mid-chord, and trailing edge. (2) Various straight lines cutting the original foil at selected points were introduced over certain ranges of the foil. The areas of the foil above the lines were then deleted leaving the desired flat spots. (3) It was felt that offsets at various stations along the chord could be in error in its construction. When the completed section is formed, the skin would smooth over or fair these variations in offsets leaving a series of valleys and hills on the foil surface. The resulting washboard is designated as warping. To this end, a few sinusoidal

oscillations of different amplitudes and ranges were added to the original foil geometry.

In Figure 1, a list is given of the various distortions investigated. Their analytic generation is indicated. The generation of the basic NACA 16 section may be found in Reference 3. In all cases except flattening, the function defining a distortion was applied normal to the chord. If $Y(x)$ is the curve defining the contour of the basic section, $Y_N(x) = Y(x) + \Delta Y_N(x)$ gives the new profile. In the cases of flattening, new offsets were generated by straight lines, $Y_N(x) = k_0 \frac{x}{c} + k_1$, where k_0 and k_1 were determined by specifying the intersections of the lines with the foil contour. Where fairing was necessary for smoothness of the resulting profile, the old and new portions of the profile were joined by polynomial expressions. Figures 2, 3, and 4 are graphic displays of the resulting sections. In order to visually resolve some of the smaller distortions, the offsets are magnified by a constant factor as indicated.

The velocity of the fluid being very sensitive to the second derivative of the curve defining the foil geometry, special care was taken in creating a distorted section to insure that the second derivative of the resulting curve was kept continuous and as small as possible. This was achieved by using a large number of stations in defining the body and by fairing the distortions into the body. For example, suppose that the undistorted foil geometry is given by a curve C. If it is desired to replace some portion of the curve C with a new curve D, considerable attention must be given in joining the ends of the curve D with the original curve C. Generally, the

two points of junction of the curve C with D will exhibit discontinuous first derivatives. Thus, the new foil geometry will have two sharp discontinuities which will result in singularities in the velocity of the flow and accordingly inordinately low pressures. In order to obtain more realistic results, having restricted the theory to potential flow, such discontinuities were analytically smoothed so that non-potential effects such as separation would not be expected. It is not suggested that such discontinuities do not occur in practice, but rather that, limited to potential theory, the pressure obtained at discontinuities would be unrealistic. In addition to this, the viscous boundary layer could be of such thickness as to mask the discontinuity. For these reasons, only systematic and continuous distortions are introduced in this study.

SOLUTION OF PROBLEM

For steady, incompressible, irrotational flow of an inviscid fluid, Bernoulli's equation is

$$gh + \frac{P}{\rho} + \tfrac{1}{2}v^2 = \text{Constant.}$$

The constant may be determined from the conditions at infinity, that is, for a sufficiently large distance from the foil section:

$$P = P_\infty \text{ and } v = U.$$

Thus $1 - \frac{v^2}{U^2} = \frac{P-P_\infty}{\frac{1}{2}\rho U^2} \equiv C_P$.

Now for cavitation inception, the local pressure P is vapor pressure, P_v. Also $P_v \cong 0$ and P_∞ may be written as:

$$P_\infty(h) = P_A + \rho gh.$$

Then at cavitation inception,

$$C_{P_i} = \frac{-P_\infty(h)}{\frac{1}{2}\rho U_i^2}$$

while on the distorted section

$$C_{P_i} + \Delta C_{P_i} = \frac{-P_\infty(h)}{\frac{1}{2}\rho(U_i + \Delta U_i)^2},$$

whence

$$\frac{\Delta U_i}{U_i} = \sqrt{\frac{C_{P_i}}{C_{P_i} + \Delta C_{P_i}}} - 1,$$

giving the fractional change in cavitation inception velocity. Although the pressure distribution was calculated over the entire section for each distortion, only the lowest pressures due to the distortion are presented in this paper. These pressures are in turn compared with what they would have been on the undistorted section. This is the manner in which $\frac{\Delta U_i}{U_i}$ shall be used.

It is apparent that for an undistorted NACA 16-X08; X = .390 section with $|\alpha| \leq 2^\circ$, the lowest pressure on the section will be very near the leading edge. This is also true for all the distorted sections for the size of distortions considered in this study. Furthermore, the change in pressure on the leading edge was not appreciable for distortions not located near or on the leading edge. In order to illustrate the effect of the various distortions, a chordwise comparison of the local minimum pressure peaks on the distorted section was made with pressures calculated on the reference section. Two parameters were utilized to describe the characteristics of a distortion of any shape. First $\frac{\Delta t}{c}$ the maximum deviation from the original contour, and x/c, the chordwise location of the local minimum pressure resulting from the distortion. It should be noted that the same distortions applied at various

positions along the contour of the section will not result in the same change in pressure. Since the curvature of the section is continuously varying with the chordwise position, a constant deformation will give rise to a change in pressure which is chordwise dependent.

For general types of distortions, the pressure distribution calculated was similar to the pressure distribution of the reference section; that is, there were no additional low peaks in the pressure where the maximum distortions occurred. However, noticeable changes were calculated for the minimum pressures on the distorted section. These minimum pressures were located approximately in the same chordwise location as were the minimum pressures on the reference section for all angles of incidence.

For flat distortions, there were additional local minimum pressure peaks superimposed on the original pressure distribution at both locations where the flat portion of the contour joined the original foil contour. The low pressure peaks developed rather sharply at the local minimum.

In the case of warping the lowest pressure developed at the maximum positive deviation from the reference contour. Since the warping consisted of a series of valleys and hills on the contour, the pressure increased and decreased in a quasi-sinusoidal manner over the warped portion of the foil. The low peaks in pressure were rather flat in comparison with low pressure peaks developed in flattening.

For negative angles of incidence, the forward stagnation point of the flow moves to the upper surface of the foil and the minimum pressure is near the leading edge on the lower surface of the foil. This results in relatively

high pressures on the upper surface of the foil. Moreover for $\alpha \leq -2^{o}$, the C_p calculated for the distortions, which in all cases were applied to the upper surface of the foil, became positive so that no upper surface cavitation would be predicted. In some cases, the C_p obtained was such a small negative value that no cavitation would be predicted for a free stream velocity less than about 100 knots. This is the reason that $\left(\frac{\Delta U_i}{U_i}; \alpha\right)$ curves end at approximately -2.0^{o}.

Figure 5 is a plot of the cavitation inception velocity U_i as a function of the angle of incidence α for two depths of submergence. This plot is for the basic NACA 16 section. Each point on the curve is at a different chord location. The values represent the absolute minimum pressures calculated for the section. For this particular reference section, the minimum pressure at zero angle of incidence is located at about 60 per cent of the chord (measured from the leading edge) and moves rapidly to the leading edge for increasing angles of incidence.

The resulting changes in cavitation inception velocity for general distortions are displayed in Figures 6 and 7, plotting $\frac{\Delta U_i}{U_i}$ as a function of α. A positive $\frac{\Delta U_i}{U_i}$ indicates an increase in cavitation inception velocity, while a negative $\frac{\Delta U_i}{U_i}$ indicates a decrease. Each point of the curves is at a different chord location and corresponds nearly to the same point of minimum pressure for the undistorted section for a given angle of incidence. Each curve is plotted for a given value of $\frac{\Delta t}{c}$.

Figures 8 and 9 show U_i as a function of x/c for various angles of incidence. A submergence depth of 10' was used in the calculations for free

stream pressure. The values of U_i are those calculated only on the upper surface of the undistorted section between the leading edge and mid-chord. For any given velocity, the portion of the foil below a particular α-curve is predicted cavitation free at that angle of incidence, while the portion of the foil above the particular α-curve is cavitating. These curves may be used in conjunction with various $\left(\frac{\Delta U_i}{U_i}, \alpha\right)$ plots to establish the reduction in cavitation inception velocity at various chord locations for warping and flattening types of distortions.

Figures 10 through 13 give the results of flattening. The plots give $\frac{\Delta U_i}{U_i}$ as a function of α. These calculations were made using the lowest local pressure developed due to the flattening. The curves are plotted in pairs corresponding to the fore and aft locations of the local minimum pressure obtained from the flat portion. Such pairs of curves are plotted for various values of $\frac{\Delta t}{c}$. Figure 13 gives $\frac{\Delta U_i}{U_i}$ as a function of $\frac{\Delta t}{c}$ for various values of α, where the flat portions of the foil ended in approximately the same chordwise location.

Figures 14 through 16 give the results of warping. The $\left(\frac{\Delta U_i}{U_i}; \alpha\right)$ plots are handled in the same way as the cases of flattening. In Figure 16, $\frac{\Delta U_i}{U_i}$ was plotted as a function of $\frac{\Delta t}{c}$ for two chord locations where the maximum warping was located in nearly the same position along the chord. These calculations are plotted for various angles of incidence. In these plots, it is to be noted that only the local minimum pressures due to warping were used in the computation for the plots.

The plots of $(U_i ; \alpha)$ and $(U_i ; x/c)$ contain certain assumptions which ought to be clarified. A single depth of submergence is specified and the free surface is neglected. Also, the vapor pressure is assigned the value zero and temperature is ignored. (This is somewhat justifiable if one notes that at $20^{\circ}C$ the vapor pressure of water is 17 mm of Hg whereas atmospheric pressure is 760 mm of Hg) For these reasons, the U_i plots should not be considered to have absolute significance in determining cavitation inception velocity. The plots are added in this work for purposes of comparison. The $\left(\frac{\Delta U_i}{U_i}; \alpha \right)$ or $\left(\frac{\Delta U_i}{U_i}; x/c \right)$ plots are the essential results presented. The expression for $\frac{\Delta U_i}{U_i}$ contains only the ratio of the critical pressure coefficients of the distorted foils to the undistorted foil.

DISCUSSION OF RESULTS

In the case of general distortions, it can be seen that the only reduction in cavitation inception velocity occurred in the approximate range $-2^{o} \leq \alpha \leq +1^{o}$ and that beyond this range an actual increase in inception velocity was calculated. For the cases that the section was thickened at the mid-chord, a $\frac{\Delta t}{c} = .010$ resulted in a 9.5% reduction in inception velocity at about zero angle of incidence. For a 10' chord this is 1.2" and for a 4' chord a .48" variation. At a submergence depth of 13', the cavitation inception velocity on the undistorted section is 52.5 knots, so that the velocity is reduced by 5.0 knots. Under the same conditions, a $\frac{\Delta t}{c} = .001$ gives a 1.1% reduction in velocity or only about 0.6 knot. It thus appears that this type of distortion will not profoundly affect the performance of the foil if $\frac{\Delta t}{c}$ were kept less than or equal to 0.005. In the case of bulging at the forward quarter of the chord and an indentation of the after quarter, a slightly more pronounced effect is noted. For example, at -1^{o} angle of incidence, a 14.7% reduction in cavitation inception velocity was computed for $\frac{\Delta t}{c} = 0.005$. This corresponds to .60" on a 10' chord or .24" on a 4' chord. Here the inception velocity is reduced from 53.5 knots to 45.6 knots if the submergence depth is 13'. Under the same conditions with $\frac{\Delta t}{c} = .003$, the reduction in inception velocity is from 53.5 knots to 48.4 knots or a 9.6% reduction. In this case a negligible effect on the foil's performance would be noted for $\frac{\Delta t}{c}$ less than or equal 0.001.

The effect of warping is far more crucial to the performance of the foil. A reduction in the cavitation inception velocity was calculated for

the entire range of α. For example at .14 x/c with $\frac{\Delta t}{c}$ = .002, the reduction in inception velocity is 17.1% at 0^{o} angle of incidence. Under these conditions, the inception velocity on the undistorted section is 53.4 knots, so that there is a 9.1 knot reduction. Under the same conditions with $\frac{\Delta t}{c}$ = .001, a 13.1% reduction in inception velocity was calculated. This amounts to a 7.0 knot reduction. Figure 16 shows that for warping in this example $\frac{\Delta t}{c}$ should be kept less than 0.0005 in order to keep the cavitation inception velocity within 4 knots below 53.4 knots.

A further point should be noted about Figure 16. The distortions were generated in such a way that $\frac{\Delta t}{c}$ / $\frac{\Delta x}{c}$ was kept constant. $\frac{\Delta x}{c}$ is the length of a half-cycle of the warp. This was done to keep the tangent to the curve defining the warping about the same order of magnitude for any $\frac{\Delta t}{c}$. Thus as $\frac{\Delta t}{c}$ becomes smaller, $\frac{\Delta x}{c}$ becomes shorter. The distortions thus vary more rapidly over a given segment but their amplitude is smaller.

Flattening is equally as critical to foil performance as warping. For $\frac{\Delta t}{c}$ = .0077, a 30.0% reduction in cavitation inception velocity was calculated at 0^{o} angle of incidence and at mid-chord. Under these conditions, the inception velocity on the undistorted section was 49.5 knots. This gives a 14.9 knot reduction in velocity. For this value of $\frac{\Delta t}{c}$ there would be a maximum deviation of .925" on a 10' chord or .396" on a 4' chord. At about .10 x/c, this same value of $\frac{\Delta t}{c}$ gives a 39.3% reduction in cavitation inception velocity. At this chord position, the inception velocity for the undistorted section is 54.6 knots, so that the inception velocity is reduced by 21.4 knots. This amount of flattening is excessive and would probably never be experienced; however, it does establish an

upper bound to the effect of flattening. With $\frac{\Delta t}{c} = .0033$, the reduction in cavitation inception velocity is 16.3% at .10 x/c and at an angle of incidence of 0^{o}. This is an 8.9 knot reduction in velocity. At the same chord position and angle of incidence with $\frac{\Delta t}{c} = .00087$, a 6.8% reduction in velocity was calculated. This amounts to 3.7 knots. This distortion corresponds to .104" on a 10' chord and .040" on a 4' chord. These calculations indicate that in the case of flattening $\frac{\Delta t}{c}$ should not exceed .0008 in order not to reduce the cavitation inception velocity by more than 4 knots. It should also be noted that for flattening with $\frac{\Delta t}{c} = .0004$ the reduction in cavitation inception velocity is at most 6.0% for $\alpha \leq 0^{o}$. For negative angle of incidence, the reduction in velocity does not exceed 10.0%. For negative angle of incidence, however, the cavitation inception velocity on the undistorted section is increasing much more readily with decreasing angle of incidence than is the fractional change in cavitation velocity due to flattening. Thus, for negative angles of incidence, a 10% reduction in inception velocity is not too significant since the cavitation inception velocity is fairly high. It appears then that $\frac{\Delta t}{c} = .0004$ gives a lower bound for which negligible effects on foil performance are produced. This value of $\frac{\Delta t}{c}$ is a .048" variation in a 10' chord or .020" in a 4' chord.

Further information may be obtained from the graphs in the following manner, first classify the distortion as warping, etc. Find the variation in the contour, that is $\frac{\Delta t}{c}$, and its general chordwise location, or in the case of flattening the chordwise locations where the flattened portion of the foil joins the unvaried contour. Then with this information and a

specified angle of incidence a $\frac{\Delta U_i}{U_i}$ can be found. This number in conjunction with Figures 8 and 9 will give the reduction in cavitation inception velocity.

These calculations should not be rigidly applied to an arbitrary section since the calculations are limited to variation of a NACA 16-X08, X = .390. The calculations can be estimates of the behavior of foil sections similar to the 16-X08.

TYPE OF DISTORTION	RANGE OF DISTORTION x/c	MAXIMUM $\left\|\frac{\Delta t}{c}\right\|$	ANALYTIC EXPRESSION FOR DISTORTION	LOCATION OF $\frac{\Delta t}{c}$ MAX (x/c)	FIGURE
GENERAL	$0.00 \leq x/c \leq 1.000$	.001	$\Delta Y_N = .001 \sin [\pi x/c]$	(+) @ .5000	2b
GENERAL	$0.00 \leq x/c \leq 1.000$	.010	$\Delta Y_N = .01 \sin [\pi x/c]$	(+) @ .5000	2a
GENERAL	$0.00 \leq x/c \leq 1.000$	.003	$\Delta Y_N = .003 \sin [2\pi x/c]$	(+) @ .250 and (-) @ .750	2d
GENERAL	$0.00 \leq x/c \leq 1.000$	.005	$\Delta Y_N = .005 \sin [2\pi x/c]$	(+) @ .250 and (-) @ .750	2c
FLATTENING	$0.15 \leq x/c \leq .50$	.005491	$Y_N = k_0\, x/c + k_1$	(-) @ .31658	3
FLATTENING	$0.10 \leq x/c \leq .50$	.007774	$Y_N = k_0\, x/c + k_1$	(-) @ .28533	3a
FLATTENING	$0.00066 \leq x/c \leq .110$	.003282	$Y_N = k_0\, x/c + k_1$	(-) @ .04280	3b
FLATTENING	$0.065 \leq x/c \leq .150$	.000869	$Y_N = k_0\, x/c + k_1$	(-) @ .10483	3c
FLATTENING	$0.450 \leq x/c \leq 0.550$	.000401	$Y_N = k_0\, x/c + k_1$	(-) @ .5000	3c
FLATTENING	$0.350 \leq x/c \leq 0.450$	.0003998	$Y_N = k_0\, x/c + k_1$	(-) @ .40108	3b
WARPING	$.09833 \leq x/c \leq .49833$ SUB-RANGE 0.10 x/c	.002	$\Delta Y_N = .002 \sin \frac{4\pi(x/c - .09833)}{.4}$	(+) @ .14833 (-) .24833 (+) @ .34833 (-) .44833	4
WARPING	$.09833 \leq x/c \leq .49833$ SUB-RANGE 0.05 x/c	.001	$\Delta Y_N = .001 \sin \frac{8\pi(x/c - .09833)}{.4}$	(+) @ .12333 (-) .17333 (+) @ .22333 (-) .27333 (+) @ .32333 (-) .37333 (+) @ .42333 (-) .47333	4a

Notes (1) For flattening k_0, k_1 may be determined from the offsets.

(2) The analytic expressions do not contain the fairing functions.

Figure 1

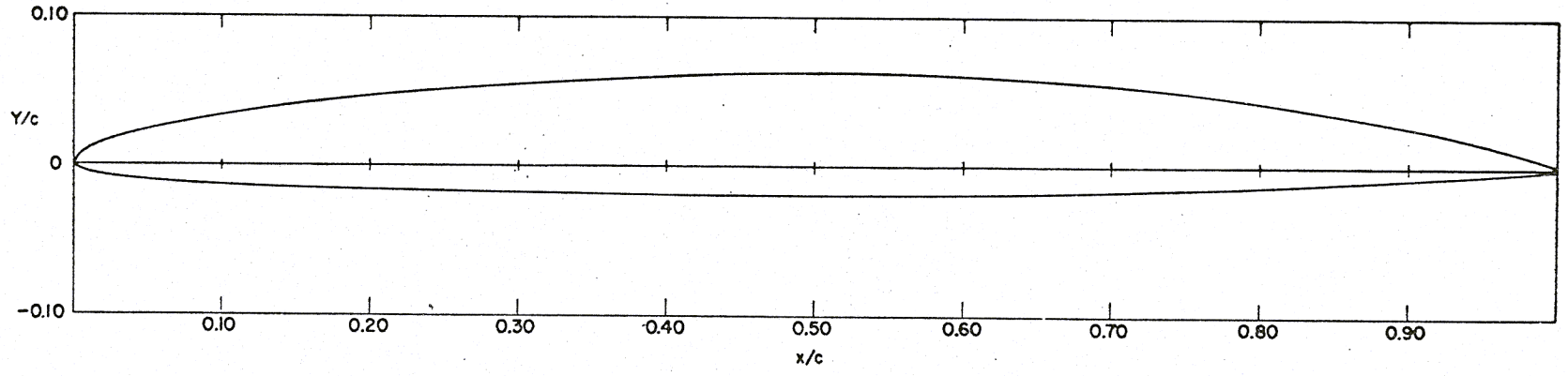

Figure 2 The NACA 16-X08; X = .390 Section

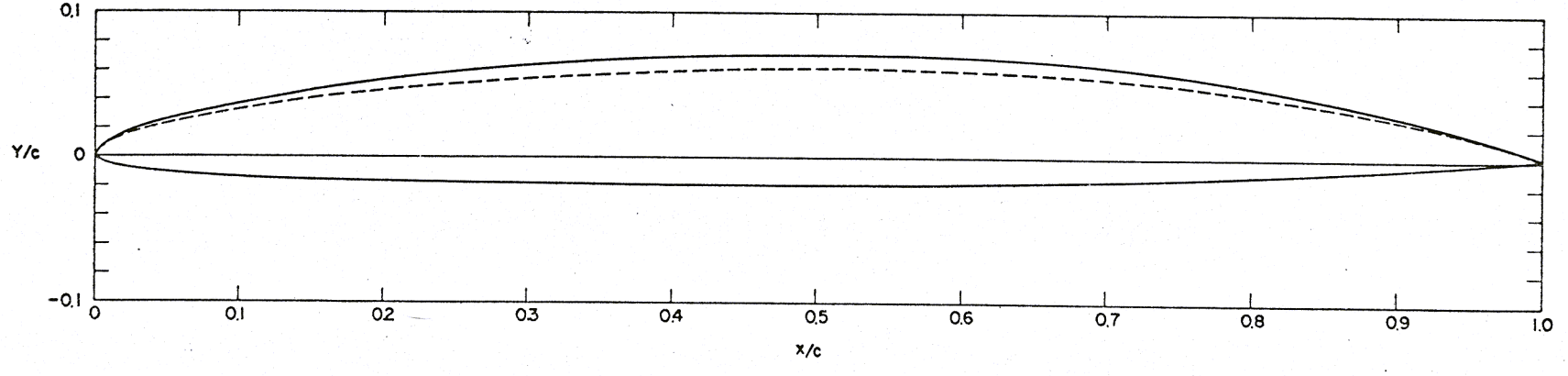

Figure 2a – Example of a General Distortion with $\frac{\Delta t}{c} = .010$

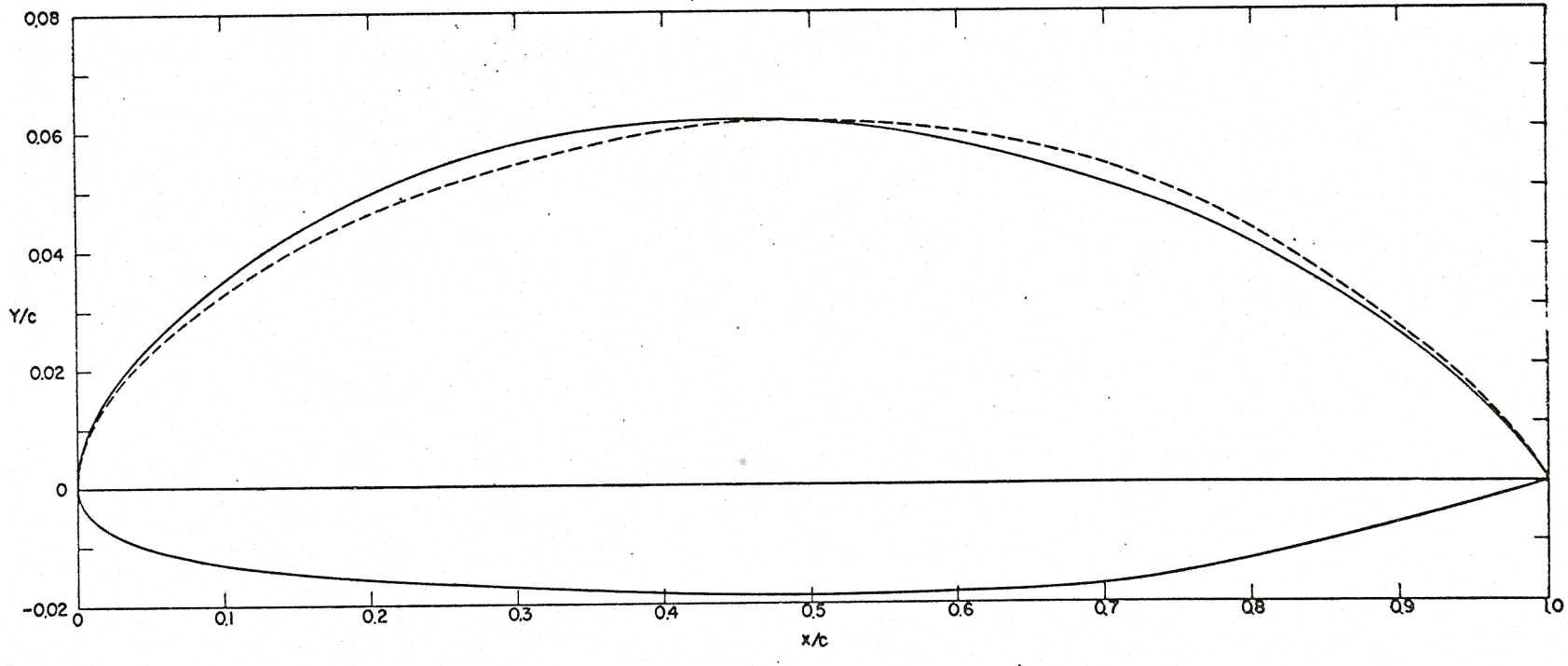

Figure 2d – Example of General Distortion with $\frac{\Delta t}{c} = .003$

(Ordinate magnified by four)

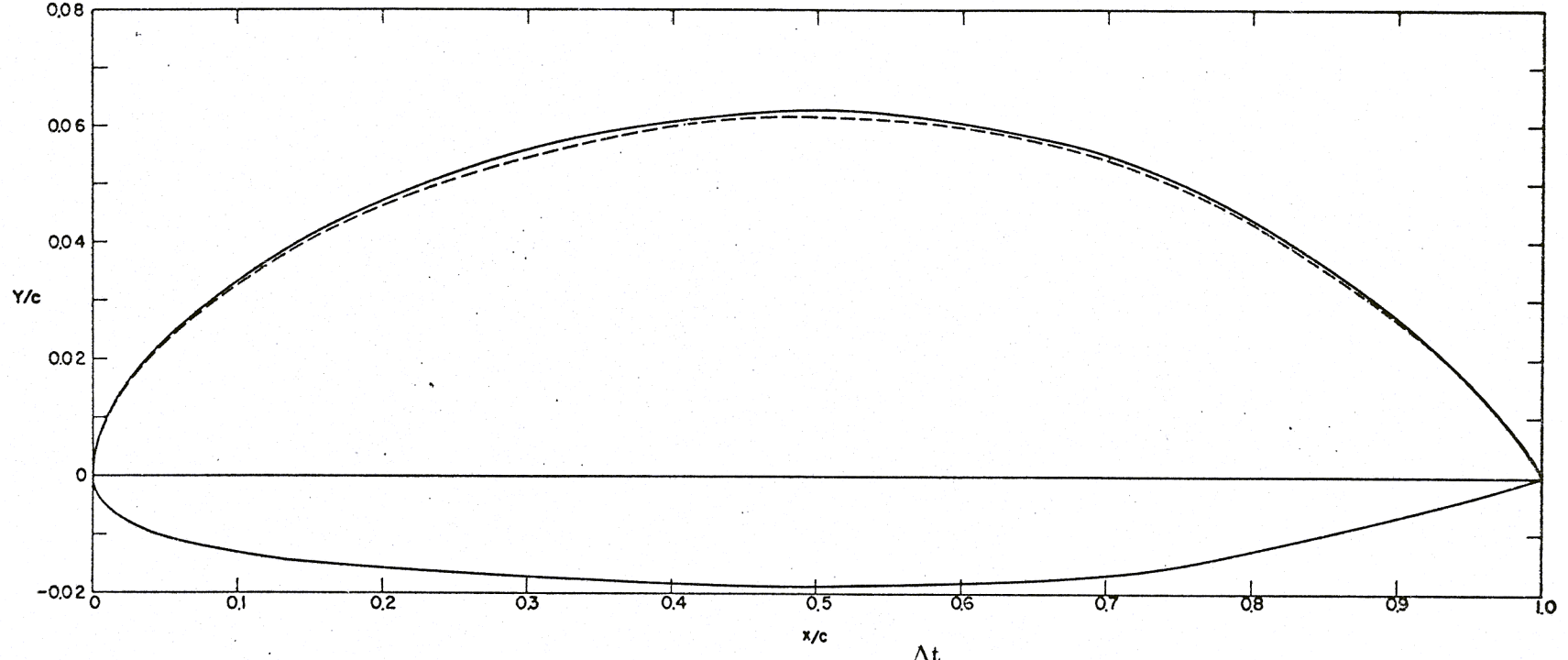

Figure 2b – Example of a General Distortion with $\frac{\Delta t}{c} = .001$ (Ordinate magnified by four)

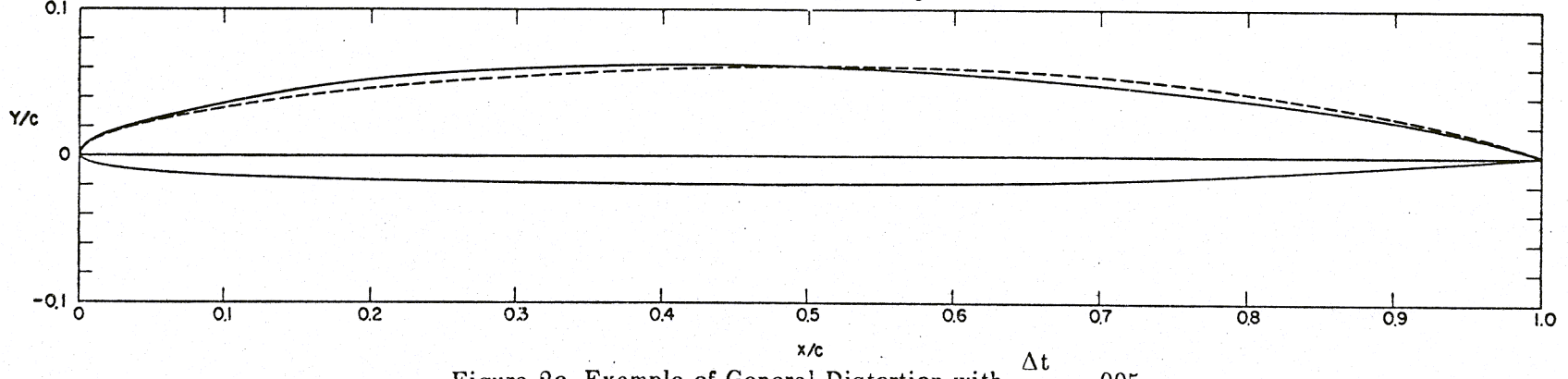

Figure 2c-Example of General Distortion with $\frac{\Delta t}{c} = .005$